

On a new class of score functions to estimate tail probabilities of some stochastic processes with adaptive multilevel splitting

Cite as: Chaos 29, 033126 (2019); <https://doi.org/10.1063/1.5081440>

Submitted: 14 November 2018 . Accepted: 26 February 2019 . Published Online: 19 March 2019

Charles-Edouard Bréhier , and Tony Lelièvre 



View Online



Export Citation



CrossMark



Don't let your writing keep you from getting published!

AIP | Author Services

Learn more today!



On a new class of score functions to estimate tail probabilities of some stochastic processes with adaptive multilevel splitting

Cite as: Chaos 29, 033126 (2019); doi: 10.1063/1.5081440

Submitted: 14 November 2018 · Accepted: 26 February 2019 ·

Published Online: 19 March 2019



View Online



Export Citation



CrossMark

Charles-Edouard Bréhier^{1,a)}  and Tony Lelièvre^{2,b)} 

AFFILIATIONS

¹Univ Lyon, CNRS, Université Claude Bernard Lyon 1, UMR5208, Institut Camille Jordan, F-69622 Villeurbanne, France

²Université Paris-Est, CERMICS (ENPC), INRIA, 6-8-10 Ave. Blaise Pascal, 77455 Marne-la-Vallée, France

Note: This article is part of the Focus Issue on “Rare Event Sampling Methods: Development, Analysis and Application.”

^{a)}brehier@math.univ-lyon1.fr

^{b)}lelievre@cermics.enpc.fr

ABSTRACT

We investigate the application of the adaptive multilevel splitting algorithm for the estimation of tail probabilities of solutions of stochastic differential equations evaluated at a given time and of associated temporal averages. We introduce a new, very general, and effective family of score functions that is designed for these problems. We illustrate its behavior in a series of numerical experiments. In particular, we demonstrate how it can be used to estimate large deviations rate functionals for the longtime limit of temporal averages.

Published under license by AIP Publishing. <https://doi.org/10.1063/1.5081440>

The simulation of rare events is a challenging computational issue that appears in many fields of science and engineering. This article is devoted to the design and the mathematical analysis of a new class of Monte Carlo methods, based on the adaptive multilevel splitting strategy, which has been developed in the last decade. Numerical experiments are performed to validate and illustrate our new algorithms.

I. INTRODUCTION

Fast and accurate estimation of rare event probabilities, and the effective simulation of these events, is a challenging computational issue, which appears in many fields of science and engineering. Since rare events are often the ones that matter in complex systems, designing efficient and easily implementable algorithms is a crucial question, which has been the subject of many studies in the recent years.

Since the pioneering works on Monte Carlo methods, several classes of algorithms have been developed, see, for instance, the monographs.^{3,15,41} The most popular strategies are importance sampling and splitting. On the one hand, importance sampling consists of changing the probability distribution, such that under the new

probability distribution, the events of interest are not rare anymore. Appropriate reweighting then yields consistent estimators. This strategy has, for instance, been applied recently to simulate rare events in climate models.³⁷ On the other hand, splitting techniques consist of writing the rare event probability as a product of conditional probabilities which are simpler to estimate, and in using interacting particle systems in order to estimate these conditional probabilities.

In this article, a class of splitting algorithms is considered. Splitting techniques have been introduced in the 1950s²⁹ and have been extensively studied in the last two decades.^{16,20,25,26} Many variants have appeared in the literature: generalized multilevel splitting,^{6,7} RESTART,^{47,48} Subset simulation,⁴ Nested sampling,^{43,44} Reversible shaking transformations with interacting particle systems,^{1,27} genealogical particle analysis,^{21,49} etc.

The adaptive multilevel splitting (AMS) algorithm¹⁸ is designed to estimate rare event probabilities of the type $\mathbb{P}(\tau_B < \tau_A)$, where τ_A and τ_B are stopping times associated with a Markov process X , typically the entrance times of X in regions A and B of the state space. In many applications, A and B are metastable states for the process. The algorithm is based on selection and mutation mechanisms, which leads to the evolution of a system of interacting replicas. The selection is performed using a score function, which is often referred to as a reaction coordinate when dealing with metastable systems. We refer

to Sec. III B for a precise algorithmic description, but let us first recall the role of the score function, which is the principal object studied in this article. The score function is chosen by the user and is denoted by ξ in the following. It is defined on the state space of the process, it is real-valued, and it allows one to measure the “distance” to the target set B . It is assumed that there exists z_{\max} such that $\xi(x) > z_{\max}$ for all $x \in B$. Each replica in the algorithm is a trajectory of the process, stopped when entering A or B ; the score of the replica is the maximum of the score function over this trajectory. Iteratively, the replicas with the lowest scores are removed, and the replicas with largest scores are duplicated (using some statistically consistent procedure). As will become clear from the discussion below, the expectation of the estimator of the probability obtained by AMS is exactly $\mathbb{P}(\tau_B < \tau_A)$ (the estimator is unbiased) whatever the choice of the score function. This enables easy parallelization of the code: one can consider the average of the estimators obtained with independent runs of AMS to reduce the statistical variance. However, the variance (and thus the statistical error) of the estimator highly depends on the score function. The choice of the score function thus has a huge impact on the practical efficiency of the algorithm. It is desirable to design families of score functions that are both general and effective.

The objective of this article is to design and test new score functions, using the AMS strategy, to estimate probabilities of the type $\mathbb{P}[\Phi(X_T) > a]$ or $\mathbb{P}\left[\frac{1}{T} \int_0^T \phi(X_t) dt > a\right]$, where a is a threshold, Φ and ϕ are real-valued functions, and $(X_t)_{0 \leq t \leq T}$ is a Markov process. In fact, as will be explained below, the probabilities of interest can be rewritten as $\mathbb{P}(\tau_B < \tau_A)$, associated with an auxiliary Markov process. Our main contribution is the identification of appropriate score functions related to this interpretation and which return a non-zero value for the estimator of the probability of interest. By using then an AMS algorithm which fits in the Generalized Adaptive Multilevel Splitting framework,¹¹ one can construct unbiased estimators of the probability (and possibly of other quantities of interest).

The efficiency of the approach is investigated with numerical experiments, using several test cases taken from the literature on rare events. First, validation is performed on one-dimensional Gaussian models (Brownian Motion,⁴⁶ Ornstein-Uhlenbeck process⁴⁹). More complex test cases then illustrate the efficiency of the approach and of the new score functions introduced in this article: drifted Brownian Motion, three-dimensional Lorenz model.^{5,32} Estimations of probabilities depending on temporal averages $\frac{1}{T} \int_0^T \phi(X_s) ds$ are also considered for two models:²⁴ the one-dimensional Ornstein-Uhlenbeck process and a driven periodic diffusion. In these examples, values of large deviations rate functionals for the longtime limit $T \rightarrow \infty$ are estimated.

In the last decade, many works have been devoted to the analysis and applications of AMS algorithms. A series of work has been devoted to the analysis of the so-called ideal case,^{9,13,14,28} namely, when the AMS algorithm is applied with the optimal score function (namely, the so-called committor function). In practice, this optimal score function is unknown. Beyond the ideal case, consistency¹¹ (unbiasedness of the small probability estimator) and efficiency¹⁷ (variance of the small probability estimator) have been studied. Moreover, the adaption of the original algorithm to the discrete-in-time setting has been studied in detail in Ref. 11. It can be used to compute transition times between metastable states,¹⁹ return times,³⁰

or other observables associated with the rare event of interest.³⁴ The AMS algorithm has been successfully applied in many contexts: the Allen-Cahn stochastic partial differential equation,^{12,39} the simulation of Bose-Einstein condensates,³⁶ molecular dynamics and computational chemistry,^{2,19,31,45} nuclear physics,^{33–35} and turbulence,^{8,38} for example.

This article is organized as follows. Section II presents the precise mathematical setting, in particular, the rare event probability of interest is defined by (7). A general formulation of the AMS algorithm designed to estimate this quantity is provided in Sec. III, in particular, see Sec. III B for the full algorithmic description. Examples of appropriate score functions are discussed in Sec. IV. To overcome the limitations of a vanilla strategy, Sec. IV A, our main contribution is the construction of the score functions presented in Sec. IV B. Finally, numerical experiments are reported in Sec. V.

II. SETTING

We consider stochastic processes, with values in \mathbb{R}^d , in dimension $d \in \mathbb{N}$, which are solutions of Stochastic Differential Equations (SDEs) of the type for $0 \leq t_0 \leq t \leq T$ and $x_0 \in \mathbb{R}^d$

$$dX_t^{t_0, x_0} = f(t, X_t^{t_0, x_0}) dt + \sigma(t, X_t^{t_0, x_0}) dW(t), \quad (1)$$

where $X_t^{t_0, x_0} \in \mathbb{R}^d$, with the initial condition

$$X_{t_0}^{t_0, x_0} = x_0. \quad (2)$$

The noise $[W(t)]_{t \geq 0}$ is given by a standard Wiener process with values in \mathbb{R}^D , for some $D \in \mathbb{N}$. The coefficients $f : [0, T] \times \mathbb{R}^d \rightarrow \mathbb{R}^d$ and $\sigma : [0, T] \times \mathbb{R}^d \rightarrow \mathbb{R}^{d \times D}$ are assumed to be sufficiently smooth to ensure global well-posedness of the SDE.

In this work, two types of rare events associated with $(X_t^{t_0, x_0})_{0 \leq t \leq T}$ are considered. Let $a \in \mathbb{R}$ denote a threshold, and let $\Phi, \phi : \mathbb{R}^d \rightarrow \mathbb{R}$ be two measurable functions. First, we are interested in tail probabilities for the random variable $\Phi(X_T^{t_0, x_0})$, namely, in

$$\mathbb{P}[\Phi(X_T^{t_0, x_0}) > a]. \quad (3)$$

Second, we are interested in tail probabilities for temporal averages, which is defined as

$$\mathbb{P}\left[\frac{1}{T - t_0} \int_{t_0}^T \phi(X_t^{t_0, x_0}) dt > a\right]. \quad (4)$$

We will investigate numerically the performance of AMS estimators for both (3) and (4) on various examples. In particular, we will consider the regime $T \rightarrow \infty$ for (4) in order to estimate large deviations rate functionals.

Note that the case of temporal averages (4) can be rewritten in the form of (3). Indeed, the probability (4) may be written as (3) for the auxiliary process defined by $\tilde{X}_t^{t_0, x_0} = (X_t^{t_0, x_0}, Y_t^{t_0, x_0})$, where $Y_t^{t_0, x_0} = \phi(x_0)$, and for $t > t_0$

$$Y_t^{t_0, x_0} = \frac{1}{t - t_0} \int_{t_0}^t \phi(X_s^{t_0, x_0}) ds$$

and with $\tilde{\Phi}(x, y) = y$. The process $(Y_t^{t_0, x_0})_{t_0 \leq t \leq T}$ is the solution of the following ordinary differential equation (ODE):

$$dY_t^{t_0, x_0} = \frac{1}{t - t_0} [\phi(X_t^{t_0, x_0}) - Y_t^{t_0, x_0}], \quad t > t_0, \quad Y_{t_0}^{t_0, x_0} = \phi(x_0)$$

coupled with the SDE for the diffusion process $(X_t^{t_0, x_0})_{t_0 \leq t \leq T}$. This trick will be used for our numerical experiments below. Therefore, in the following, we present the AMS algorithm and discuss its theoretical properties only for (3).

For future purposes, observe that the target probability (3) may be written as $u_a(t_0, x_0)$, where

$$u_a(t, x) = \mathbb{P}[\Phi(X_T^{t,x}) > a] \tag{5}$$

is the solution (under appropriate regularity assumptions) of the backward Kolmogorov equation

$$\begin{cases} \frac{\partial u_a(t,x)}{\partial t} + \mathcal{L}_t u_a(t,x) = 0 & \text{for } t \in [0, T] \text{ and } x \in \mathbb{R}^d, \\ u_a(T, x) = \mathbb{1}_{\Phi(x) > a} & \text{for } x \in \mathbb{R}^d, \end{cases} \tag{6}$$

where the infinitesimal generator \mathcal{L}_t is defined by: for all test functions φ , $\mathcal{L}_t \varphi(x) = f(t, x) \cdot \nabla \varphi(x) + \frac{1}{2} \sigma(t, x) \sigma(t, x)^* : \nabla^2 \varphi(x)$. Approximating the solutions of PDEs of this type using deterministic methods is in general possible only when the dimension d is small. Instead, Monte Carlo methods may be used. However, naive Monte Carlo algorithms are not efficient in the rare event regime, e.g., when $a \rightarrow \infty$ or when the diffusion coefficient is of the type $\sigma_\epsilon = \sqrt{\epsilon} \sigma$ and $\epsilon \rightarrow 0$.

In practice, discrete-time approximations are implemented. Let $\Delta t > 0$ denote the time step size of the integrator (for instance, the standard Euler-Maruyama method), with $T = N\Delta t$ and $t_0 = n_0 \Delta t$, where $n_0 \in \mathbb{N}_0, N \in \mathbb{N}, n_0 \leq N$. With a slight abuse of notation, let us denote the discrete-time process obtained after discretization of (1) by $(X_n^{n_0, x_0})_{n_0 \leq n \leq N}$. The time-discrete counterpart of (3) is then

$$\mathbb{P}[\Phi(X_N^{n_0, x_0}) > a]. \tag{7}$$

The algorithms presented below are used to estimate probabilities of the type (7).

Remark 1. *It is assumed that the initial condition is deterministic: $X_{n_0}^{n_0, x_0} = x_0$. The adaptation of the algorithms presented below to the case of a random initial condition is straightforward, by simply using the Markov property: $\mathbb{P}[\Phi(X_N) > a] = \int \mathbb{P}[\Phi(X_N^{n_0, x_0}) > a] d\mu_0(x_0)$, where μ_0 denotes the law of X_{n_0} .*

Remark 2. *Instead of using an integrator with time step size Δt , one may use an integrator with a smaller time step size δt (such that $\frac{\Delta t}{\delta t} \in \mathbb{N}$) to define the discrete-time process. This does not change the general presentation of the algorithm. The question of the choice of Δt and δt in practice is not trivial and highly depends on the model under study. In the numerical experiments below (Sec. V), it is always assumed that $\delta t = \Delta t$.*

III. GENERAL FORMULATION OF THE ADAPTIVE MULTILEVEL SPLITTING ALGORITHM

A. Context

The goal is to estimate the probability p given by (7), in the regime where p is small, which is, for example, the case when a is large.

It is convenient to introduce an auxiliary process $(Z_n)_{n_0 \leq n \leq N}$ such that $Z_n = (n\Delta t, X_n^{n_0, x_0})$. Indeed, let

$$A = \{(T, x); \Phi(x) \leq a\}, \quad B = \{(T, x); \Phi(x) > a\}$$

and define the associated stopping times

$$\begin{aligned} \tau_A &= \inf \{n \geq n_0, n \in \mathbb{N}_0; Z_n \in A\}, \\ \tau_B &= \inf \{n \geq n_0, n \in \mathbb{N}_0; Z_n \in B\}. \end{aligned}$$

Then, the probability p given by (7) can be rewritten as

$$p = \mathbb{P}[\Phi(X_N^{n_0, x_0}) > a] = \mathbb{P}(\tau_B < \tau_A). \tag{8}$$

We are then in a position to build algorithms that fit in the Generalized Adaptive Multilevel Splitting framework developed in Ref. 11, which ensures that the obtained estimators of the probability (8) are unbiased.

For that, a score function, or reaction coordinate, ξ , needs to be given. Following the above interpretation, ξ may depend on $z = (n\Delta t, x)$.

To run the algorithm and define simple unbiased estimators of p , only one requirement is imposed on the function ξ : there exists ξ_{\max} such that

$$B \subset \{z; \xi(z) > \xi_{\max}\},$$

which in the context of this article is rephrased as

$$\Phi(x) > a \implies \xi(T, x) > \xi_{\max}. \tag{9}$$

The principle of the splitting algorithm is then to write

$$\begin{aligned} \mathbb{P}(\tau_B < \tau_A) &= \mathbb{P}(\tau_{\zeta_1} < \tau_A) \mathbb{P}(\tau_{\zeta_2} < \tau_A | \tau_{\zeta_1} < \tau_A) \\ &\times \mathbb{P}(\tau_{\zeta_3} < \tau_A | \tau_{\zeta_2} < \tau_A) \cdots \mathbb{P}(\tau_B < \tau_A | \tau_{\xi_{\max}} < \tau_A) \end{aligned}$$

for an increasing sequence of levels $(\zeta_q)_{q \geq 1}$, where $\tau_\zeta = \inf\{n \geq n_0; \xi(Z_n) > \zeta\}$. If the levels are well chosen, then the successive conditional probabilities $\mathbb{P}(\tau_{\zeta_{q+1}} < \tau_A | \tau_{\zeta_q} < \tau_A)$ are easy to compute. The principle of the adaptive multilevel splitting algorithm¹⁸ is to choose the levels adaptively, so that the successive conditional probabilities $\mathbb{P}(\tau_{\zeta_{q+1}} < \tau_A | \tau_{\zeta_q} < \tau_A)$ are constant and fixed. The levels constructed in the algorithm are then random.

B. The adaptive multilevel splitting algorithm

Before giving the detailed algorithm, let us roughly explain the main steps (we also refer to Ref. 11 for more details and intuition on the algorithm). In the initialization, one samples n_{rep} trajectories following (1) and (2) and compute the score of each trajectory, namely, the maximum of ξ attained along the path. Then, the algorithm proceeds as follows: one discards the trajectory that has the smallest score and in order to keep the number of trajectories fixed, a new one is created by choosing one of the remaining trajectories at random, copying it up to the score of the killed trajectory, and sampling the end of trajectory independently from the past. This is called the partial resampling. One thus obtains a new ensemble of n_{rep} trajectories on which one can iterate by again discarding the trajectory which has the smallest score. As the iteration goes, one thus obtains trajectories with larger and larger scores, and an estimate of the probability of interest is obtained as $(1 - 1/n_{\text{rep}})^{Q_{\text{iter}}} P(\tau_B < \tau_A | \tau_{\xi_{\max}} < \tau_A)$ [note that $(1 - 1/n_{\text{rep}})$ is an estimate of the conditional probability to reach level ζ_{q+1} conditionally to the fact that level ζ_q has been reached], where Q_{iter} is the number of iterations required to reach the maximum level ξ_{\max} . In practice, $P(\tau_B < \tau_A | \tau_{\xi_{\max}} < \tau_A)$ is estimated by the

proportion of trajectories that reach B before A at the last iteration of the algorithm, namely, when all the trajectories satisfy $\tau_{\xi_{\max}} < \tau_A$.

Actually, the algorithm has to be adapted in order to take into account situations when more than one particle has the smallest score, which happens with non-zero probability for Markov chains. Let us now give the details of the AMS algorithm.

To simplify notation, in the sequel, the initial condition x_0 and the time n_0 are omitted in the notation of the replicas.

- (a) *Input*
 - $n_{\text{rep}} \in \mathbb{N}$, the number of replicas,
 - a score function $z = (n\Delta t, x) \mapsto \xi(n\Delta t, x) \in \mathbb{R}$ and a stopping level $\xi_{\max} \in \mathbb{R}$ such that (9) is satisfied.
- (b) *Initialization*
 - Sample n_{rep} independent realizations of the Markov process

$$X^j = (X_m^j)_{n_0 \leq m \leq N}, \quad 1 \leq j \leq n_{\text{rep}}$$
 following the dynamics (1) and (2).
 - Compute the score of each replica, $M^j = \max_{n_0 \leq m \leq N} \xi(m\Delta t, X_m^j)$.
 - Compute the level $\mathcal{Z} = \min_{1 \leq j \leq n_{\text{rep}}} M^j$.
 - Define $\mathcal{K} = \{j \in \{1, \dots, n_{\text{rep}}\}; M^j = \mathcal{Z}\}$.
 - Set $q = 0, \hat{p} = 1, \mathcal{B} = 1$.
- (c) *Stopping criterion* If $\mathcal{Z} \geq \xi_{\max}$ or $\text{card}(\mathcal{K}) = n_{\text{rep}}$, then set $\mathcal{B} = 0$.
- (d) *while* $\mathcal{B} = 1$
 - **Update**
 - $q \leftarrow q + 1$ and $\hat{p} \leftarrow \hat{p} \cdot (1 - \frac{\text{card}(\mathcal{K})}{n})$.
 - **Splitting**
 - Reindex the replicas, such that

$$\begin{cases} M^j = \mathcal{Z} & \text{if } j \in \{1, \dots, \text{card}(\mathcal{K})\}, \\ M^j > \mathcal{Z} & \text{if } j \in \{\text{card}(\mathcal{K}) + 1, \dots, n_{\text{rep}}\}. \end{cases}$$
 - For replicas with index $j \in \{1, \dots, \text{card}(\mathcal{K})\}$, sample labels $\ell_1, \dots, \ell_{\text{card}(\mathcal{K})}$, independently and uniformly in $\{\text{card}(\mathcal{K}) + 1, \dots, n_{\text{rep}}\}$.
 - **Partial resampling**
 - Remove the replicas with label $j \in \{1, \dots, \text{card}(\mathcal{K})\}$.
 - For $j \in \{1, \dots, \text{card}(\mathcal{K})\}$, define $m_j = \inf\{m \in \{n_0, \dots, N\}; \xi(X_m^{\ell_j}) > \mathcal{Z}\}$.
 - For $m \in \{n_0, \dots, m_j\}$, set $X_m^j = X_m^{\ell_j}$.
 - Sample a new trajectory $(X_m^j)_{m_j \leq m \leq N}$ with the Markov dynamics (1) driven by independent realizations of the Brownian motion.
 - **Level computation**
 - Compute the scores $M^j = \max_{n_0 \leq m \leq N} \xi(m\Delta t, X_m^j)$.
 - Compute the level $\mathcal{Z} = \min_{1 \leq j \leq n_{\text{rep}}} M^j$.
 - Define the set $\mathcal{K} = \{j \in \{1, \dots, n_{\text{rep}}\}; M^j = \mathcal{Z}\}$.
- (e) *Stopping criterion* If $\mathcal{Z} \geq \xi_{\max}$ or $\text{card}(\mathcal{K}) = n_{\text{rep}}$, then set $\mathcal{B} = 0$.
- (f) *End while*
- (g) *Update:* $\hat{p} \leftarrow \hat{p} \frac{1}{n_{\text{rep}}} \sum_{j=1}^{n_{\text{rep}}} \mathbb{1}_{\Phi(X_N^j) \geq a}$.
- (h) *Output:* \hat{p} and $Q_{\text{iter}} = q$.

Remark 3. We presented the algorithm in its simplest form. There are many variants, see Ref. 11. For example, the killing level

\mathcal{Z} can be defined as $\mathcal{Z} = M^{(k)}$ where $M^{(1)} \leq M^{(2)} \leq \dots \leq M^{(n_{\text{rep}})}$ denotes an increasing relabeling of the scores $(M^j)_{1 \leq j \leq n_{\text{rep}}}$ (order statistics).

C. Consistency result

Let \hat{p} and Q_{iter} be the outputs of the realization of the above algorithm. We quote the following result,¹¹ which states that the output \hat{p} of the algorithm described in Sec. III B is an unbiased estimator of the probability given by (7).

Theorem 1. Let ξ be a score function and $\xi_{\max} \in \mathbb{R}$ be such that (9) is satisfied. Let $n_{\text{rep}} \in \mathbb{N}$ be a given number of replicas. Assume that almost surely the algorithm stops after a finite number of iterations: $Q_{\text{iter}} < \infty$ almost surely.

Then, \hat{p} is an unbiased estimator of the probability p given by (8)

$$\mathbb{E}[\hat{p}] = \mathbb{P}[\Phi(X_N^{n_0, x_0}) > a].$$

Note that if $\psi : \mathbb{R}^d \rightarrow \mathbb{R}$ is a function with support included in $\{x; \Phi(x) > a\}$, i.e., $\psi(x) = 0$ if $\Phi(x) \leq a$, then an unbiased estimator of $\mathbb{E}[\psi(X_N^{n_0, x_0})]$ is given by replacing the final update in the above algorithm [see step (g)], by

$$\hat{p} \leftarrow \hat{p} \frac{1}{n_{\text{rep}}} \sum_{j=1}^{n_{\text{rep}}} \psi(X_N^j).$$

The unbiasedness property is crucial in practice for the following two reasons. First, it is very easy to parallelize the estimation of rare events using this property. Indeed, since the estimator is unbiased whatever the value of n_{rep} , to obtain a convergent estimation, one has to simply fix n_{rep} to a value that enables the computation of \hat{p} on a single CPU, and then to sample M independent realizations of this \hat{p} , run in parallel. In the large M limit, one obtains a convergent estimator of the quantity of interest by simply considering the average of the realizations of \hat{p} . Second, the practical interest of Theorem 1 is that since $\mathbb{E}(\hat{p})$ is the same whatever the choice of the numerical parameters (namely, n_{rep} and ξ), one can compare the results obtained with different choices to get confidence in the result. For example, one can consider the confidence intervals obtained with M independent realizations of \hat{p} for two different choices of ξ , and check whether these confidence intervals overlap or not.

Remark 4. In the algorithm described in Sec. III B, the set \mathcal{K} defined in the initialization and in the level computation steps may have a cardinal strictly larger than 1, even if the level \mathcal{Z} is defined as the minimum of the scores over the replicas. This simply means that more than one replica has a score that is the smallest among the replicas. In the discrete-time setting (namely, for Markov chains), this occurs with non-zero probability, and it requires an appropriate modification of the original AMS algorithm, as described above, see Ref. 11 for more details.

Note that in particular, there is a possibility that the algorithm stops if $\text{card}(\mathcal{K}) = n_{\text{rep}}$, in which case there is an extinction of the system of replicas.

IV. CHOICES OF THE SCORE FUNCTION

Let us now describe the various score functions we will consider in order to estimate (7).

A. Vanilla score function and limitations

The simplest choice consists of choosing the score function as given by

$$\xi_{\text{std}}(n\Delta t, x) = \Phi(x) \tag{10}$$

with $\xi_{\text{max}} = a$. In this case, the score function does not depend on the time variable.

If the conditional probability

$$q = \mathbb{P} \left[\Phi(X_N^{n_0, x_0}) > a \mid \max_{n_0 \leq n \leq N} \Phi(X_n^{n_0, x_0}) > a \right]$$

is small, the performance of this vanilla strategy may be poor. Indeed, only a small proportion of the replicas have a non-zero contribution to the value of the estimator of the probability (7). It may even happen that all the replicas satisfy $\max_{n_0 \leq n \leq N} \Phi(X_n^{n_0, x_0}) > a$ but that none of them satisfies $\Phi(X_N^{n_0, x_0}) > a$. In that situation, the algorithm returns $\hat{p} = 0$ to estimate $p > 0$. One of the goals of this work is to construct score functions that circumvent that issue: with the score functions introduced below, almost surely $\hat{p} \neq 0$.

Let us illustrate the limitation of the vanilla score function on a straightforward example. Assume that the initial condition x_0 of the process satisfies $\Phi(x_0) > a$, then $\max_{n_0 \leq n \leq N} \Phi(X_n^{n_0, x_0}) > a$ with probability 1. Thus, the conditional probability q is equal to p . In such a case, applying the AMS algorithm using the vanilla score function is equivalent to applying the crude Monte Carlo method (the stopping criterion is satisfied right after the initialization, where independent replicas are used). In this situation, the vanilla score function is obviously ineffective, and new score functions need to be designed.

B. Time-dependent score functions

As discussed above, it is natural to design score functions ξ , which satisfy the following condition:

$$\{\Phi(X_N^{n_0, x_0}) > a\} = \left\{ \max_{n_0 \leq n \leq T} \xi(n\Delta t, X_n^{n_0, x_0}) > 1 \right\}. \tag{11}$$

The choice of the value $\xi_{\text{max}} = 1$ on the right-hand side above is arbitrary, but no generality is lost. Indeed, if a score function ξ satisfying (11) is used in the above AMS algorithm, with $\xi_{\text{max}} = 1$, at the last update, the ratio $\left(\frac{1}{n_{\text{rep}}}\right) \sum_{j=1}^{n_{\text{rep}}} \mathbb{1}_{\Phi(X_N^j) \geq a}$ is identically equal to 1, since all replicas satisfy $\max_{n_0 \leq n \leq T} \xi(n\Delta t, X_n^{n_0, x_0}) > 1$. In particular, by construction $\hat{p} \neq 0$ (provided $Q_{\text{iter}} < \infty$).

As will be seen below, in practice it is more natural to identify functions $\tilde{\xi}$ taking values in $(-\infty, 1]$, which satisfy the condition

$$\{\Phi(X_N^{n_0, x_0}) > a\} = \left\{ \max_{n_0 \leq n \leq T} \tilde{\xi}(n\Delta t, X_n^{n_0, x_0}) = 1 \right\}, \tag{12}$$

instead of (11). To justify the use of the algorithm in this case, observe that $\tilde{\xi}(t, x) = \xi(t, x) + \mathbb{1}_{\tilde{\xi}(t, x) = 1}$ then satisfies (11). In addition, when running the algorithm, choosing either $\tilde{\xi}$ or ξ exactly yields the same result. We are thus in the setting where the unbiasedness result of Theorem 1 applies. The score functions presented below will satisfy (12) instead of (11).

One of the novelties of this article is the introduction of the following score function:

$$\xi_{\text{new}}(n\Delta t, x) = [\Phi(x) - a] \mathbb{1}_{\Phi(x) \leq a} + \frac{n\Delta t}{N\Delta t} \mathbb{1}_{\Phi(x) > a}. \tag{13}$$

Observe that ξ_{new} takes values in $(-\infty, 1]$, and that $\xi_{\text{new}}(n\Delta t, x) = 1$ if and only if $n = N$ and $\Phi(x) \geq a$. Thus, the condition (12) is satisfied. We refer to Fig. 1 for a schematic representation of this score function.

Note that the score function defined by (13) only depends on the function Φ , on the threshold a , and on the final time $T = N\Delta t$. It may thus be applied in any situation, but in some cases better score functions may be built upon using more information on the dynamics. The practical implementation is very simple.

Let us explain how the AMS algorithm proceeds when used with the score function (13). Observe that

$$\left\{ \max_{n_0 \leq n \leq N} \xi_{\text{new}}(n\Delta t, X_n^{n_0, x_0}) \geq 0 \right\} = \left\{ \max_{n_0 \leq n \leq N} \Phi(X_n^{n_0, x_0}) > a \right\}.$$

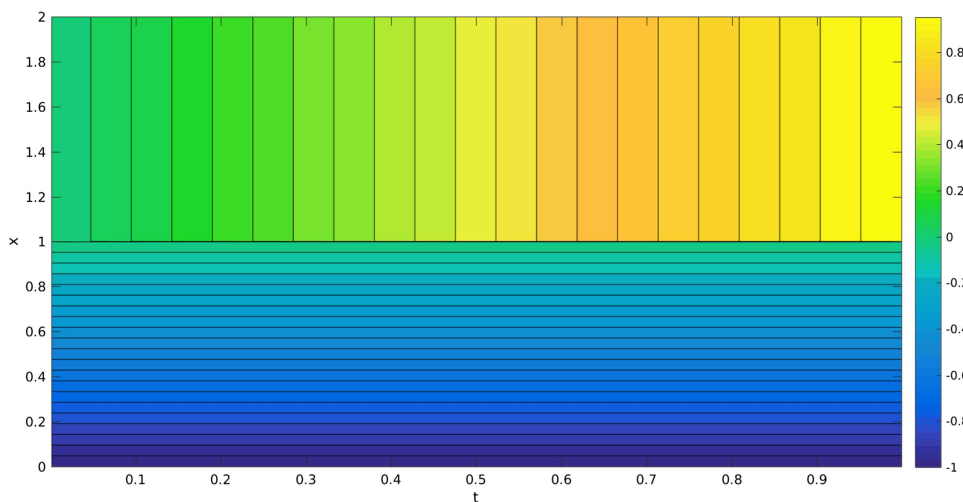


FIG. 1. Level lines of the score function $(t, x) \mapsto \xi_{\text{new}}(t, x)$, with $\Phi(x) = x$, $a = 1$, $T = 1$.

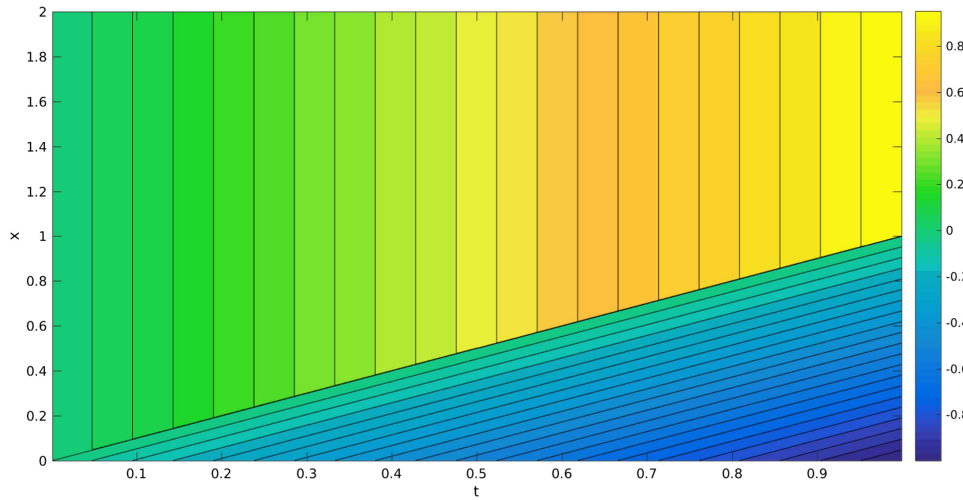


FIG. 2. Level lines of the score function $(t, x) \mapsto \xi_{\text{new}}^a(t, x)$, with $\mathbf{a}(t) = atT^{-1}$, and $\Phi(x) = x, a = 1, T = 1$.

The first iterations of the algorithm, up to reaching level 0, are thus devoted to construct n_{rep} replicas, which satisfy the weaker condition $\left\{ \max_{n_0 \leq n \leq N} \Phi(X_n^{n_0, x_0}) > a \right\}$. In other words, if the stopping level ξ_{max} in the algorithm is set equal to 0 instead of 1, one thus recovers the vanilla AMS algorithm described above, applied with the score function $\xi(t, x) = \Phi(x)$ (independent of time t).

Compared with the vanilla score function, the AMS algorithm with the new score function does not stop when $\left\{ \max_{n_0 \leq n \leq N} \Phi(X_n^{n_0, x_0}) > a \right\}$. In terms of splitting, one can observe that this consists of writing

$$\mathbb{P}[\Phi(X_N^{n_0, x_0}) > a] = \mathbb{P}\left[\Phi(X_N^{n_0, x_0}) > a \mid \max_{n_0 \leq n \leq N} \Phi(X_n^{n_0, x_0}) > a\right] \times \mathbb{P}\left[\max_{n_0 \leq n \leq N} \Phi(X_n^{n_0, x_0}) > a\right],$$

and the remaining effort consists of estimating the above conditional probability.

More generally, one can observe that for every $n_1 \in \{n_0, \dots, N\}$,

$$\left\{ \max_{n_0 \leq n \leq N} \xi_{\text{new}}(n\Delta t, X_n^{n_0, x_0}) \geq \frac{n_1}{N} \right\} = \left\{ \max_{n_1 \leq n \leq N} \Phi(X_n^{n_0, x_0}) > a \right\}.$$

The construction of the score function (13) is associated with the following family of nested events:

$$\begin{aligned} & \left\{ \max_{n_0 \leq n \leq N} \xi_{\text{new}}(n\Delta t, X_n^{n_0, x_0}) \geq 1 \right\} \\ & \subset \dots \subset \left\{ \max_{n_0 \leq n \leq N} \xi_{\text{new}}(n\Delta t, X_n^{n_0, x_0}) \geq \frac{n_1}{N} \right\}, \\ & \subset \dots \subset \left\{ \max_{n_0 \leq n \leq N} \xi_{\text{new}}(n\Delta t, X_n^{n_0, x_0}) \geq 0 \right\}, \end{aligned}$$

which equivalently may be rewritten as

$$\begin{aligned} \left\{ \Phi(X_N^{n_0, x_0}) > a \right\} & \subset \dots \subset \left\{ \max_{n_1 \leq n \leq N} \Phi(X_n^{n_0, x_0}) > a \right\}, \\ & \subset \dots \subset \left\{ \max_{n_0 \leq n \leq N} \Phi(X_n^{n_0, x_0}) > a \right\}. \end{aligned}$$

In the selection procedure, the intervals $[n_1 \Delta t, N \Delta t]$ are iteratively reduced (by increasing the left end point of the interval), until they ultimately contain only the point $N \Delta t$ (the right end point of the interval that remains fixed).

To conclude, we mention that the construction given by (13) can be generalized as follows. Let $\mathbf{a} : [0, T] \rightarrow \mathbb{R}$ be a non-decreasing function, such that $\mathbf{a}(T) = a$. Define

$$\xi_{\text{new}}^a(n\Delta t, x) = [\Phi(x) - \mathbf{a}(n\Delta t)] \mathbb{1}_{\Phi(x) \leq \mathbf{a}(n\Delta t)} + \frac{n\Delta t}{N\Delta t} \mathbb{1}_{\Phi(x) > \mathbf{a}(n\Delta t)}. \tag{14}$$

The score function ξ_{new} defined by (13) is a particular case of (14), with $\mathbf{a}(t) = a$. Optimizing the choice of the function \mathbf{a} may help improve the efficiency of the algorithm. Note that condition (12) is satisfied with $\xi = \xi_{\text{new}}^a$. We refer to Fig. 2 for a schematic representation of this score function.

C. The optimal score function: The committor function

For the general setting presented in Sec. III A where one wants to estimate $\mathbb{P}(\tau_B < \tau_A)$, the committor function is defined as $z \mapsto \mathbb{P}^z(\tau_B < \tau_A)$, where the superscript z refers to the initial condition of the process Z . In Ref. 17, it is shown that, in a continuous-time setting, the asymptotic variance (as the number of replicas n_{rep} goes to infinity) of the AMS algorithm is minimized when using the committor function as the score function. It is thus interesting to look at what the committor function looks like in our context. Note that it is also shown in Corollary 2.9 of Ref. 17 that the average number of iterations of AMS is of the order $-n_{\text{rep}} \log(p)$ whatever the choice of the score function: this is why we only concentrate on the scaling in p of the variance, depending on the choice of the score function. For

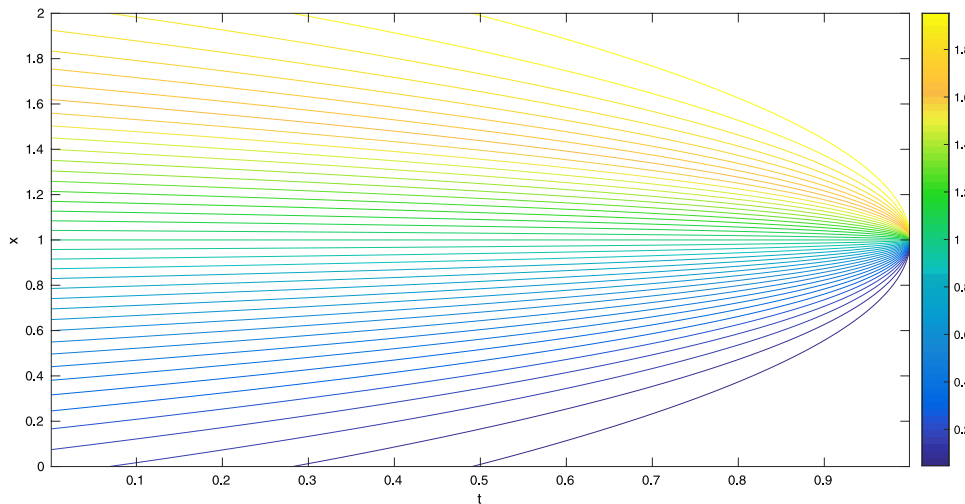


FIG. 3. Level lines of the committor function $(t, x) \mapsto \xi_{\text{com}}(t, x)$, in the Brownian Motion case $X(t) = B(t)$, with $a = 1$ and $T = 1$.

the optimal score function, namely, the committor function, the variance scales like $-p^2 \log(p)$, see Corollary 2.8 in Ref. 17, whereas for bad committor functions, one can get twice the variance of a brute force Monte Carlo, namely, $2p$.

In our context, the committor function is given by

$$\xi_{\text{com}}(n\Delta t, x) = \mathbb{P}[\Phi(X_N^{n,x}) > a]. \tag{15}$$

For the discussion, it is more convenient to consider the continuous-time version $\xi_{\text{com}}(t, x) = \mathbb{P}[\Phi(X_T^{t,x}) > a]$, for $t \in [0, T]$, that we still denote ξ_{com} with a slight abuse of notation. Recall that $u_a(t, x) = \mathbb{P}[\Phi(X_T^{t,x}) > a] = \xi_{\text{com}}(t, x)$ satisfies the Kolmogorov backward equation (6), as explained in Sec. II.

As mentioned above, the asymptotic variance (as the number of replicas n_{rep} goes to infinity) of the AMS algorithm is minimized when using the committor function as the score function.¹⁷ The asymptotic variance is then $\frac{-p^2 \log(p)}{n_{\text{rep}}}$, where p is the probability that is estimated. The analysis of the AMS algorithm in the ideal case, i.e., when using the committor function as the score function, has been performed in many works.^{9,13,14,28}

Of course, in practice, the committor function is unknown and the asymptotic variance depends on the chosen score function. It has been proved¹⁷ that the asymptotic variance is always bounded from above by $\frac{2p(1-p)}{n_{\text{rep}}}$, for any choice of the score function, where we recall that the asymptotic variance of the vanilla Monte Carlo method is $\frac{p(1-p)}{n_{\text{rep}}}$. This can be seen as a sign of the robustness of the AMS approach to estimate rare event probability (contrary to the importance sampling method, which may result in a dramatic increase in the asymptotic variance compared with the vanilla Monte Carlo method).

For simple Gaussian models, namely, when X is a Brownian Motion, an Ornstein-Uhlenbeck process, or a drifted Brownian Motion, it is possible to compute analytically the committor function. This is useful to validate algorithms on test cases, as will be illustrated in Sec. V. Figure 3 represents the level lines of the committor function for a one-dimensional Brownian Motion (with $T = 1$ and $a = 1$). In

that case,

$$\xi_{\text{com}}(t, x) = 1 - F\left(\frac{a - x}{\sqrt{T - t}}\right),$$

where F is the cumulative distribution function of the standard Gaussian distribution $\mathcal{N}(0, 1)$, to be compared to the level sets of ξ_{new} and ξ_{new}^a in Figs. 1 and 2. This form leads one to define other families of appropriate score functions

$$\xi(t, x) = 1 - F[\phi(t, x)],$$

where $\phi(t, x) \xrightarrow{t \rightarrow \infty} (-\infty)\mathbb{1}_{\Phi(x) > a} + (+\infty)\mathbb{1}_{\Phi(x) < a}$. But the efficiency depends more on the choice of ϕ . In practice, we did not observe much gain in our numerical experiments, compared to the score function ξ_{new} introduced in Sec. IV B.

Let us mention that various techniques have been proposed in order to approximate the committor function, in particular in the context of importance sampling techniques for rare events, since the committor function also gives the optimal change of measure. If diffusions with vanishing noise are considered,^{22,23,46} solutions of associated Hamilton-Jacobi equations are good candidates to estimate the committor function. See also Ref. 42 for approximations based on coarse-grained models. Whether such constructions are possible when considering temporal averages, instead of the terminal value of the process is unclear.

V. NUMERICAL SIMULATIONS

Let p denote the rare event probability of interest. An estimator of p is calculated as the empirical average over independent realizations of the AMS algorithm, given a choice of score function ξ . The main objective of this section is to investigate the behavior of the algorithm when choosing $\xi = \xi_{\text{new}}$ given by (13). A comparison with the vanilla score function $\xi = \xi_{\text{std}}$ given by (10) is provided.

Let $n_{\text{rep}} \in \mathbb{N}$ denote the number of replicas, and let $M \in \mathbb{N}$, and $(\hat{p}_m)_{1 \leq m \leq M}$ be the output probabilities of M independent realizations

of the AMS algorithm. We report the values of the empirical average

$$\hat{p} = \frac{1}{M} \sum_{m=1}^M \hat{p}_m$$

and of the empirical variance $\hat{\sigma}^2 = \frac{1}{M-1} \sum_{m=1}^M (\hat{p}_m - \hat{p})^2$. Confidence intervals are computed as

$$\left[\hat{p} - \frac{1.96\hat{\sigma}}{\sqrt{M}}, \hat{p} + \frac{1.96\hat{\sigma}}{\sqrt{M}} \right],$$

assuming that the number of realizations M is sufficiently large to use the Gaussian, Central Limit Theorem, regime.

Recall that $\mathbb{E}[\hat{p}] = \mathbb{E}[\hat{p}_1] = p$, whatever the choice of the score function ξ and of the number of replicas n_{rep} , thanks to Theorem 1. The variance of the estimator and thus the efficiency strongly depends on ξ . In the experiments below, the empirical variance $\hat{\sigma}^2$ is compared with the optimal asymptotic variance $\frac{-p^2 \log(p)}{n_{\text{rep}}}$ for (adaptive) multilevel splitting algorithms, which is obtained in the regime $n_{\text{rep}} \rightarrow \infty$, when choosing the (unknown in general) committor function $\xi = \xi_{\text{com}}$ as the score function. The difference between the empirical variance and the optimal one can be seen as a measure of how far the chosen score function is from the committor.

Recall that, as explained in Sec. IV B, it is sufficient to compare the asymptotic variances (instead of computational costs) for different choices of the score functions, since we are only interested in the behavior as p tends to 0. In this regime, for the mean number of iterations for one realization of the algorithm, the score function only plays a role in a multiplicative constant.

In some of the numerical experiments below, the conditional probability

$$q = \mathbb{P} \left[\Phi(X_N) > a \mid \max_{0 \leq n \leq N} \Phi(X_n) > a \right] \quad (16)$$

is also estimated by

$$\hat{q} = \frac{\hat{p}}{\hat{p}_{\text{max}}},$$

where $\hat{p}_{\text{max}} = \frac{1}{M} \sum_{m=1}^M \hat{p}_{\text{max},m}$ is the estimator of the probability

$$p_{\text{max}} = \mathbb{P} \left[\max_{0 \leq n \leq N} \Phi(X_n) > a \right], \quad (17)$$

which is estimated using the vanilla score function $\xi = \xi_{\text{std}}$.

A. Validation using two Gaussian models

In this section, we validate the AMS algorithm with various score functions on simple models for which the probability of the rare event is known with arbitrary precision.

1. Brownian motion

We follow here numerical experiments from Ref. 46. Let $d = 1$ and consider the diffusion process given by

$$dX(t) = \sqrt{2\beta^{-1}} dW(t), \quad X(0) = 0.1,$$

where $[W(t)]_{t \geq 0}$ is a standard real-valued Wiener process.

The dynamics is discretized using the explicit Euler-Maruyama method, with time step size $\Delta t = 10^{-3}$ (note that the numerical scheme gives here the exact solution)

$$X_{n+1} = X_n + \sqrt{2\beta^{-1} \Delta t} \zeta_n$$

with $X_0 = X(0) = 0.1$, where $(\zeta_n)_{0 \leq n \leq N}$ are independent standard Gaussian random variables.

The goal is to estimate the probability

$$p = \mathbb{P}(|X_N| > 1).$$

This corresponds to the choice $\Phi(x) = |x|$, $a = 1$, $T = 1$ so that $N = T/\Delta t = 10^3$.

Since $X(t) = X(0) + W(t)$, the law of $X(t)$ is a Gaussian distribution, and the value of $\mathbb{P}(|X(1)| \geq 1)$ can be computed exactly in terms of the cumulative distribution function of the standard Gaussian distribution.

In the numerical experiment reported in Table I, the number of replicas is set equal to $n_{\text{rep}} = 10^3$, and the empirical average is computed over $M = 10^3$ independent realizations of the algorithm.

This numerical experiment validates the algorithm using $\xi = \xi_{\text{new}}$ in the case of a one-dimensional Brownian Motion. The empirical variance $\hat{\sigma}^2$ is much smaller than $\frac{p(1-p)}{n_{\text{rep}}}$, which would be obtained using a naive Monte Carlo strategy (using n_{rep} independent replicas). It is observed that the ratio between the empirical and the optimal variances increases when p decreases, but in practice this increase only has a limited impact and the new algorithm remains effective.

TABLE I. Brownian Motion, $n_{\text{rep}} = 10^3$, $M = 10^3$.

β	\hat{p}	$p (\Delta t = 0)$	Confidence interval	$\hat{\sigma}^2$	$\frac{-p^2 \log(p)}{n_{\text{rep}}}$
2	3.196×10^{-1}	3.197×10^{-1}	$[3.188 \times 10^{-1}, 3.203 \times 10^{-1}]$	1.362×10^{-4}	1.166×10^{-4}
4	1.617×10^{-1}	1.614×10^{-1}	$[1.612 \times 10^{-1}, 1.621 \times 10^{-1}]$	5.456×10^{-5}	4.751×10^{-5}
8	4.983×10^{-2}	4.983×10^{-2}	$[4.963 \times 10^{-2}, 5.002 \times 10^{-2}]$	9.815×10^{-6}	7.447×10^{-6}
16	6.411×10^{-3}	6.386×10^{-3}	$[6.371 \times 10^{-3}, 6.451 \times 10^{-3}]$	4.242×10^{-7}	2.061×10^{-7}
32	1.634×10^{-4}	1.645×10^{-4}	$[1.614 \times 10^{-4}, 1.655 \times 10^{-4}]$	1.063×10^{-9}	2.358×10^{-10}
64	1.800×10^{-7}	1.782×10^{-7}	$[1.740 \times 10^{-7}, 1.860 \times 10^{-7}]$	9.360×10^{-15}	4.935×10^{-16}
128	3.045×10^{-13}	3.011×10^{-13}	$[2.426 \times 10^{-13}, 3.664 \times 10^{-13}]$	9.986×10^{-25}	2.614×10^{-27}

TABLE II. Ornstein-Uhlenbeck, $T = 8$. Comparison of the new and the vanilla splitting algorithms. $n_{\text{rep}} = 10^2$, $M = 10^4$.

a	\hat{p}_{new}	\hat{p}_{std}	$p(\Delta t = 0)$	$\hat{\sigma}_{\text{new}}^2$	$\hat{\sigma}_{\text{std}}^2$	$\frac{-p^2 \log(p)}{n_{\text{rep}}}$	\hat{r}
2.8	3.792×10^{-5}	3.714×10^{-5}	3.751×10^{-5}	1.696×10^{-9}	2.435×10^{-9}	1.434×10^{-10}	0.54
2.9	2.036×10^{-5}	2.071×10^{-5}	2.055×10^{-5}	5.439×10^{-10}	8.289×10^{-10}	4.557×10^{-11}	0.51
3.0	1.103×10^{-5}	1.128×10^{-5}	1.104×10^{-5}	1.843×10^{-10}	2.745×10^{-10}	1.392×10^{-11}	0.49
3.1	5.915×10^{-6}	5.968×10^{-6}	5.824×10^{-6}	5.599×10^{-11}	8.457×10^{-11}	4.089×10^{-12}	0.47
3.2	2.978×10^{-6}	3.022×10^{-6}	3.013×10^{-6}	1.639×10^{-11}	2.368×10^{-11}	1.154×10^{-12}	0.43

2. Ornstein-Uhlenbeck

We consider here an example taken from Ref. 49. Let $d = 1$ and consider the diffusion process given by

$$dX(t) = -X(t)dt + dW(t), \quad X(0) = 0.$$

The dynamics is discretized using the explicit Euler-Maruyama method, with time step size $\Delta t = 10^{-3}$

$$X_{n+1} = X_n - \Delta t X_n + \sqrt{\Delta t} \zeta_n,$$

with $X_0 = X(0) = 0$, where $(\zeta_n)_{0 \leq n \leq N}$ are independent standard Gaussian random variables.

In the numerical experiment reported in Table II, the goal is to estimate the probability

$$p = \mathbb{P}(X_N > a)$$

for different values of a . This corresponds to the choice $\Phi(x) = x$. The value of T is set to $T = 8$. The number of replicas is set equal to $n_{\text{rep}} = 10^2$, and the empirical average is computed over $M = 10^4$ independent realizations of the algorithm. The estimator \hat{p}_{new} of p and the empirical variance $\hat{\sigma}_{\text{new}}^2$ are obtained using the score function $\xi = \xi_{\text{new}}$. The estimator \hat{p}_{std} and the empirical variance $\hat{\sigma}_{\text{std}}^2$ are obtained using the vanilla splitting strategy, with reaction coordinate $\xi = \xi_{\text{std}}$. The value of the probability p for the continuous time process, and the optimal variance $\frac{-p^2 \log(p)}{n_{\text{rep}}}$ are also reported for comparison.

The quantity

$$\hat{r} = \frac{1}{M} \sum_{m=1}^M \mathbb{1}_{\hat{p}_m > 0}$$

is also reported, when the vanilla score function is used. This is the proportion of the independent realizations of the algorithm, which contribute in the empirical average. This proportion depends on the conditional probability q [see (16)]: it may happen that the n_{rep} replicas obtained at the final iteration all satisfy $X_N \leq 1$, even if by construction they all satisfy $\max_{0 \leq n \leq N} X_n > 1$. However, by construction (except if the extinction of the system of replicas happens, which has not been observed in this experiment), if the new score function is used, \hat{r} is identically equal to 1. Observe that, when T tends to infinity, by ergodicity of the process, $p_{\text{max}} \rightarrow 1$ [see (17) for the definition of p_{max}], whereas q and p converge to a non-trivial probability. Thus, when T tends to infinity, it is expected that \hat{r} will be equal to 0 if M is too small, when using the vanilla strategy with $\xi = \xi_{\text{std}}$. The conditional probability q is also estimated: $\hat{q} = 0.01$ (Table II).

To conclude this section, note that on this example, the AMS algorithms applied with the vanilla and the new score functions have a similar quantitative behavior in terms of asymptotic variance. However, their qualitative properties are different. When the conditional probability q is small, the advantage of the new score function is the fact that the output \hat{p} is always positive, so that even with a few realizations, one gets a rough but informative approximation of the target probability.

B. Drifted Brownian motion

We here consider numerical examples taken from Refs. 10 and 40. Let $d = 1$ and consider the diffusion process given by

$$dX_t = -\alpha dt + \sqrt{2\beta^{-1}} dW(t), \quad X(0) = 0.$$

The dynamics is discretized using the explicit Euler-Maruyama method, with time step size $\Delta t = 10^{-2}$ (which gives again the exact solution in this simple case)

$$X_{n+1} = X_n - \alpha \Delta t + \sqrt{2\beta^{-1} \Delta t} \zeta_n,$$

with $X_0 = X(0) = 0$, where $(\zeta_n)_{0 \leq n \leq N}$ are independent standard Gaussian random variables.

The goal is to estimate the probability

$$p = \mathbb{P}(X_N > 1),$$

thus $\Phi(x) = x$, $a = 1$. One considers the final time $T = 1$, so that $N = T/\Delta t = 10^2$. The value of α is set equal to $\alpha = 4$. As in the previous example, the value of p is easy to obtain using the fact that X_N is Gaussian.

As explained in Sec. IV A, if the initial condition satisfies $X(0) > 1$, the AMS algorithm with the vanilla score function is equivalent to a crude Monte Carlo algorithm to estimate the probability p , and thus it becomes ineffective in the limit $p \rightarrow 0$ (namely, in this model, α and/or T become large). The new score function is in this case mandatory to obtain reliable estimates. From now on, we focus on the case $X(0) = 0$.

In this numerical experiment, see Table III, three choices of score functions are considered. The number of replicas is $n_{\text{rep}} = 10^3$. First, the estimator \hat{p}_{new} and the empirical variance $\hat{\sigma}_{\text{new}}^2$ are obtained using $\xi = \xi_{\text{new}}$, with a sample size $M = 4 \cdot 10^4$. Second, the estimator $\hat{p}_{\text{new,a}}$ and the empirical variance $\hat{\sigma}_{\text{new,a}}^2$ are obtained using $\xi = \xi_{\text{new,a}}$ with $\mathbf{a}(t) = (\frac{at}{T})$, with a sample size $M = 4 \cdot 10^5$. Finally, the estimator \hat{p}_{std} and the empirical variance $\hat{\sigma}_{\text{std}}^2$ are obtained using $\xi = \xi_{\text{std}}$, with a sample size $M = 4 \cdot 10^4$. The sample sizes are chosen such

TABLE III. Drifted Brownian Motion, $\beta \in \{1, 2, 3, 4\}$. Comparison of two versions of the new splitting algorithm and of the vanilla splitting algorithm.

β	\hat{p}_{new}	$\hat{p}_{\text{new,a}}$	\hat{p}_{std}	p	$\hat{\sigma}_{\text{new}}^2$	$\hat{\sigma}_{\text{new,a}}^2$	$\hat{\sigma}_{\text{std}}^2$	$\frac{-p^2 \log(p)}{n_{\text{rep}}}$	\hat{r}
1	2.037×10^{-4}	2.036×10^{-4}	2.033×10^{-4}	2.035×10^{-4}	1.572×10^{-9}	5.734×10^{-9}	3.525×10^{-9}	3.519×10^{-10}	0.99
2	2.843×10^{-7}	2.870×10^{-7}	2.878×10^{-7}	2.867×10^{-7}	4.714×10^{-14}	2.348×10^{-12}	9.527×10^{-14}	1.238×10^{-15}	0.69
3	4.613×10^{-10}	4.325×10^{-10}	4.705×10^{-10}	4.571×10^{-10}	1.817×10^{-18}	2.197×10^{-17}	3.084×10^{-18}	4.493×10^{-21}	0.11
4	7.620×10^{-13}	6.975×10^{-13}	7.582×10^{-13}	7.687×10^{-13}	5.034×10^{-23}	4.388×10^{-22}	8.343×10^{-23}	1.648×10^{-26}	0.01

that the total computational cost is of the same order for the three methods.

Since the sample size is not the same for the three examples of score functions in Table III, the values of the empirical variances $\hat{\sigma}^2$ should be taken with care when comparing the methods. One would rather compare the values of $\frac{\hat{\sigma}^2}{M}$. Then, one concludes that the best performance is obtained when using $\xi = \xi_{\text{new}}^a$. The vanilla strategy, with $\xi = \xi_{\text{std}}$, seems to behave quantitatively the same as when $\xi = \xi_{\text{new}}$. However, the values of the proportion \hat{r} of realizations such that $\hat{p}_m \neq 0$ is not zero are also reported, when $\xi = \xi_{\text{std}}$ (by construction, $\hat{r} = 1$ for the first two cases). This means that if M was decreased (for instance, M of the order 10^2 for $\beta = 4$), then the output of the experiment would be $\hat{p}_{\text{std}} = 0$.

As a consequence, the new algorithm clearly overcomes the limitation of the vanilla strategy when $\xi = \xi_{\text{std}}$. However, the score functions are far from being optimal, as revealed by the comparison with the optimal variance.

C. Temporal averages for an Ornstein-Uhlenbeck process

In this section, we consider an example taken from Ref. 24. Consider the one-dimensional Ornstein-Uhlenbeck process X , which is the solution of the SDE

$$dX(t) = -X(t)dt + \sqrt{2\beta^{-1}}dW(t), \quad X(0) = 0$$

and define the temporal average

$$Y(T) = \frac{1}{T} \int_0^T X(s)ds.$$

More generally, set $Y(t) = \frac{1}{t} \int_0^t X(s)ds$, for $t \in (0, T]$ and $Y(0) = 0$.

The discretization is performed using the explicit Euler-Maruyama method, with time step size $\Delta t = 5 \cdot 10^{-3}$: for $n \in \{0, \dots, N\}$ with $N\Delta t = T$,

$$X_{n+1} = (1 - \Delta t)X_n + \sqrt{2\beta^{-1}\Delta t}\zeta_n, \quad Y_n = \frac{1}{n} \sum_{m=1}^n X_m,$$

with $X_0 = Y_0 = 0$. Note that Y satisfies a recursion formula $Y_{n+1} = [1 - (\frac{1}{n+1})]Y_n + (\frac{1}{n+1})X_{n+1}$.

The number of replicas is set equal to $n_{\text{rep}} = 10^3$ and the sample size to compute empirical averages is $M = 10^2$.

In this section, the probability that is estimated is

$$p(T, a) = \mathbb{P}(Y_N > a).$$

The associated estimator is denoted by $\hat{p}(T, a)$ and the empirical variance by $\hat{\sigma}^2(T, a)$.

In the large time limit $T \rightarrow \infty$, since the law of $Y(T)$ converges to a centered Gaussian with variance 1, $Y(T)$ satisfies a large deviation principle, with rate function I defined by: for all $a > 0$

$$\lim_{T \rightarrow \infty} -\frac{1}{T} \log \left\{ \mathbb{P}[Y(T) > a] \right\} = I(a) = \frac{a^2}{4}.$$

In the numerical experiment, we illustrate the potential of the AMS algorithm to estimate the large deviations rate function on this example. Note that in the large T limit, the probability is extremely small and in practice cannot be estimated by the vanilla splitting strategy (for the same number of replicas, and a number of independent realizations chosen such that the computational cost is the same as for the new score function, the vanilla strategy returns 0 as an estimator of the probability). The estimate of the rate function $\hat{I}(a)$ is obtained by a regression procedure (we checked that we are indeed in the regime where $\log \left\{ \mathbb{P}[Y(T) > a] \right\}$ is linear in T). In addition to statistical error, two sources of numerical error are identified: values of T may not be sufficiently large, and the discretization of the dynamics and of the computation of temporal averages introduces a bias. The results, reported in Table IV, show the interest of this approach to estimate large deviations rate functionals.

D. Lorenz model

We consider the following stochastic version of the 3-dimensional Lorenz system, see Refs. 5 and 32 for similar numerical experiments

$$\begin{cases} dX_1^\beta(t) = \sigma[X_2(t) - X_1(t)]dt + \sqrt{2\beta^{-1}}dW(t), \\ dX_2^\beta(t) = [rX_1(t) - X_2(t) - X_1(t)X_3(t)]dt, \\ dX_3^\beta(t) = X_1(t)X_2(t) - bX_3(t), \end{cases}$$

which depends on parameters σ, r, b , and β . The parameters are given the following values in this section: $\sigma = 3, r = 26$, and $b = 1$.

Consider first the deterministic case, i.e., $\beta = \infty$. Then, the system admits three unstable equilibria, and one of them is

$$x^* = [\sqrt{b(r-1)}, \sqrt{b(r-1)}, r-1] = (5, 5, 25).$$

Let the initial condition be given by $X^\infty(0) = x^* + \frac{1}{2}(1, 1, 1)$. Then, one has the following stability result:⁵ for all $t \geq 0, \Phi[X^\infty(t)] \leq 1$, where

$$\Phi(x) = \frac{x_1^2}{(r+\sigma)^2 \frac{b}{\sigma}} + \frac{x_2^2}{(r+\sigma)^2 b} + \frac{[x_3 - (r+\sigma)]^2}{(r+\sigma)^2}.$$

When noise is introduced in the system, i.e., $\beta < \infty$, we are interested in the estimation of the probability

$$\mathbb{P}\{\Phi[X^\beta(T)] > 1\}$$

TABLE IV. Temporal averages for an Ornstein-Uhlenbeck process. $n_{\text{rep}} = 10^3$ and $M = 10^2$.

a	$\hat{p}(T = 25, a)$ $\hat{\sigma}^2(T = 25, a)$	$\hat{p}(T = 50, a)$ $\hat{\sigma}^2(T = 50, a)$	$\hat{p}(T = 100, a)$ $\hat{\sigma}^2(T = 100, a)$	$\hat{p}(T = 200, a)$ $\hat{\sigma}^2(T = 200, a)$	$\hat{I}(a)$	$\frac{a^2}{4}$
0.4	7.28×10^{-2}	2.12×10^{-2}	2.22×10^{-3}	2.75×10^{-5}	0.045	0.040
...	2.02×10^{-5}	3.25×10^{-6}	1.27×10^{-7}	3.85×10^{-11}
0.6	1.45×10^{-2}	1.16×10^{-3}	1.16×10^{-5}	7.28×10^{-10}	0.096	0.090
...	1.36×10^{-6}	5.85×10^{-8}	2.21×10^{-10}	6.44×10^{-19}
0.8	1.76×10^{-3}	2.57×10^{-5}	6.12×10^{-9}	2.73×10^{-16}	0.169	0.160
...	8.01×10^{-8}	3.32×10^{-10}	1.44×10^{-16}	1.98×10^{-31}
1.0	1.37×10^{-4}	1.67×10^{-7}	3.06×10^{-13}	1.71×10^{-24}	0.261	0.250
...	1.47×10^{-9}	2.07×10^{-14}	1.16×10^{-25}	9.32×10^{-48}
1.2	6.21×10^{-6}	4.83×10^{-10}	2.71×10^{-18}	2.88×10^{-34}	0.373	0.360
...	1.40×10^{-11}	6.69×10^{-19}	3.49×10^{-35}	5.21×10^{-67}

with threshold $a = 1$.

In the numerical experiments reported in Table V, $\sqrt{2\beta^{-1}} = 3$, and the discretization is performed using the explicit Euler-Maruyama method, with time step size $\Delta t = 10^{-2}$. The sample size is $M = 10^4$, and the number of replicas is $n_{\text{rep}} = 10^3$.

This numerical experiment thus illustrates the potential of the adaptive multilevel splitting algorithms introduced in this article, for applications to complex, nonlinear, stochastic models (Table V).

E. Driven periodic diffusion

We finally consider an example taken from Ref. 24. In this section, we consider the SDE on the unit circle, i.e., on the torus \mathbb{T} ,

$$dX(t) = \{-V'[X(t)] + \gamma\}dt + \sqrt{2}dW(t),$$

where the potential energy function $V(x) = \cos(2\pi x)$ is periodic, and $\gamma \in \mathbb{R}$. If $\gamma \neq 0$, this is called a non-equilibrium process since the drift term $-V'(x) + \gamma$ is not the derivative of a function defined on the torus \mathbb{T} . In the remainder of this section, let $\gamma = 1$, and let the initial condition in the simulation be $X_0 = 0$. The discretization is performed using the Euler-Maruyama method, with time step size $\Delta t = 10^{-2}$.

We are interested in the behavior of $\frac{X_T}{T}$, when $T \rightarrow \infty$, more precisely we apply the AMS algorithm to estimate

$$p(T, a) = \mathbb{P}[X(T) > aT] = \mathbb{P}\left[\frac{X(T)}{T} > a\right].$$

TABLE V. Lorenz model. $n_{\text{rep}} = 10^3$ and $M = 10^4$.

T	\hat{p}	Confidence interval	$\hat{\sigma}^2$	$\frac{-\hat{p}^2 \log(\hat{p})}{n_{\text{rep}}}$
5	1.413×10^{-5}	$[1.388 \times 10^{-5}, 1.438 \times 10^{-5}]$	1.648×10^{-10}	2.230×10^{-12}
10	2.607×10^{-5}	$[2.534 \times 10^{-5}, 2.681 \times 10^{-5}]$	1.409×10^{-9}	7.174×10^{-12}
15	2.709×10^{-5}	$[2.609 \times 10^{-5}, 2.809 \times 10^{-5}]$	2.592×10^{-9}	7.718×10^{-12}
20	2.594×10^{-5}	$[2.484 \times 10^{-5}, 2.704 \times 10^{-5}]$	3.158×10^{-9}	7.106×10^{-12}

Following the same approach as for the temporal averages of the Ornstein-Uhlenbeck process, a large deviations rate function

$$I(a) = \lim_{T \rightarrow \infty} -\frac{1}{T} \log[p(T, a)]$$

is estimated, based on estimators of the probability $p(T, a)$ for several values of T .

In this numerical experiment, we compare two ways of applying the AMS algorithm, with the new score function ξ_{new} but with different processes: considering either the process $[X(t)]_{0 \leq t \leq T}$ with the threshold aT , or the process $[Y(t) = \frac{X(t)}{t}]_{0 < t \leq T}$, with the threshold a . Numerical values for different choices of a , T and n_{rep} , of the associated estimators $\hat{p}^X(T, a)$ and $\hat{p}^Y(T, a)$, and of the empirical variances $\hat{\sigma}^{2,X}(T, a)$ and $\hat{\sigma}^{2,Y}(T, a)$ are reported in Table VI.

It is observed that $\hat{\sigma}^{2,Y}(T, a) < \hat{\sigma}^{2,X}(T, a)$, but a fair comparison requires to take into account the (average) computational cost. Thus, the relative efficiency $\text{Eff}(Y|X)$ of using the process Y instead of X is computed as the ratio

$$\text{Eff}(Y|X) = \frac{\hat{\sigma}^{2,X} \text{comp. time}(X)}{\hat{\sigma}^{2,Y} \text{comp. time}(Y)},$$

where $\frac{\text{comp. time}(X)}{\text{comp. time}(Y)}$ is the ratio of the total computational times for the experiments using X and Y , respectively. The values of $\text{Eff}(Y|X)$ in this numerical experiment are reported in Table VI. We observe that $\text{Eff}(Y|X) > 1$ which means that the algorithm is more efficient using the process Y than the process X . To have a comparison with the committor score function, since the value of $p(T, a)$ is not known, an approximation of the optimal variance is computed using the estimator $\hat{p}^Y(T, a)$.

TABLE VI. Estimates of $\mathbb{P}(X_T > aT)$ and of $I(a)$ for the Periodic driven diffusion. The sample size is $M = 10^2$.

a	T	n_{rep}	$\hat{p}^X(T, a)$	$\hat{p}^Y(T, a)$	$\hat{\sigma}^{2,X}(T, a)$	$\hat{\sigma}^{2,Y}(T, a)$	$\frac{-[\hat{p}^Y(T, a)]^2 \log[\hat{p}^Y(T, a)]}{n_{\text{rep}}}$	Eff(Y X)	$\hat{I}(a)$
0.8	100	10^2	8.483×10^{-2}	8.489×10^{-2}	7.136×10^{-4}	2.487×10^{-4}	1.777×10^{-4}	1.0	
...	200	...	2.647×10^{-2}	2.776×10^{-2}	1.832×10^{-4}	3.519×10^{-5}	2.762×10^{-5}	1.7	0.0112
1	50	10^3	1.529×10^{-2}	1.505×10^{-2}	7.046×10^{-6}	1.513×10^{-6}	9.504×10^{-7}	3.0	
...	100	...	1.026×10^{-3}	1.085×10^{-3}	2.586×10^{-7}	3.879×10^{-8}	8.036×10^{-9}	2.8	0.0526
1.25	50	10^3	1.374×10^{-4}	1.311×10^{-4}	1.227×10^{-8}	1.355×10^{-9}	1.537×10^{-10}	4.9	
...	100	...	8.941×10^{-7}	1.017×10^{-7}	1.048×10^{-13}	1.585×10^{-15}	1.665×10^{-16}	35	0.189

Concerning the efficiency of the vanilla score function on this example, let us consider the parameters $T = 100$ and $a = 1.25$. We observe that one realization of AMS with the new score function corresponds approximately to 30 realizations of AMS with the vanilla score function, in terms of computational cost. However, over 10^4 realizations of AMS with the vanilla score function, we typically observed only realizations returning a 0 value. On the contrary, with only 10^2 realizations of AMS with the new score function yields a reliable estimate (with a good confidence interval). This clearly demonstrates the superiority of the new score function in this case.

Estimators $\hat{I}(a)$ of the large deviations rate function $I(a)$ are estimated by a regression procedure (with respect to T) using the estimators $\hat{p}^Y(T, a)$, for several values of a . The numerical values are in excellent agreement with the numerical experiments in Ref. 24. The AMS algorithm introduced in this article can thus be an efficient tool to estimate large deviations rate functions.

ACKNOWLEDGMENTS

The authors would like to thank the referees for their useful suggestions which helped improve the presentation of this article. They would also like to thank the editors of the special issue for inviting us to submit a contribution. The authors would like to thank G. Ferré and H. Touchette for discussions concerning the numerical experiments, and F. Cérou, A. Guyader, and M. Rousset for stimulating discussions at early stages of this work. The work of T. Lelièvre is supported by the European Research Council (ERC) under the European Union's Seventh Framework Programme (FP/2007-2013)/Grant Agreement No. 614492.

REFERENCES

- A. Agarwal, S. De Marco, E. Gobet, and G. Liu, "Study of new rare event simulation schemes and their application to extreme scenario generation," *Math. Comput. Simul.* **143**, 89–98 (2018).
- D. Aristoff, T. Lelièvre, C. G. Mayne, and I. Teo, "Adaptive multilevel splitting in molecular dynamics simulations," in *CEMRACS 2013—Modelling and Simulation of Complex Systems: Stochastic and Deterministic Approaches*, ESAIM Proceedings and Surveys (EDP Sciences, Les Ulis, 2015), Vol. 48, pp. 215–225.
- S. Asmussen and P. Glynn, *Stochastic Simulation: Algorithms and Analysis*, Stochastic Modelling and Applied Probability Vol. 57 (Springer, New York, 2007).
- S. K. Au and J. L. Beck, "Estimation of small failure probabilities in high dimensions by subset simulation," *J. Probab. Eng. Mech.* **16**, 263–277 (2001).
- J. L. Beck and K. M. Zuev, "Rare-event simulation," in *Handbook of Uncertainty Quantification* (Springer, 2017), pp. 1075–1100, see <https://link.springer.com/referencework/10.1007/978-3-319-11259-6>.

- Z. I. Botev and D. P. Kroese, "Efficient Monte Carlo simulation via the generalized splitting method," *Stat. Comput.* **22**(1), 1–16 (2012).
- Z. I. Botev, P. L'Ecuyer, G. Rubino, R. Simard, and B. Tuffin, "Static network reliability estimation via generalized splitting," *INFORMS J. Comput.* **25**(1), 56–71 (2013).
- F. Bouchet, J. Rolland, and E. Simonnet, "Rare event algorithm links transitions in turbulent flows with activated nucleations," *Phys. Rev. Lett.* **122**, 074502 (2019).
- C.-E. Bréhier, "Large deviations principle for the adaptive multilevel splitting algorithm in an idealized setting," *ALEA Lat. Am. J. Probab. Math. Stat.* **12**(2), 717–742 (2015).
- C.-E. Bréhier, M. Gazeau, L. Goudenège, T. Lelièvre, and M. Rousset, "Unbiasedness of some generalized adaptive multilevel splitting algorithms," e-print [arXiv:1505.02674](https://arxiv.org/abs/1505.02674), 2015.
- C.-E. Bréhier, M. Gazeau, L. Goudenège, T. Lelièvre, and M. Rousset, "Unbiasedness of some generalized adaptive multilevel splitting algorithms," *Ann. Appl. Probab.* **26**(6), 3559–3601 (2016).
- C.-E. Bréhier, M. Gazeau, L. Goudenège, and M. Rousset, "Analysis and simulation of rare events for SPDEs," in *CEMRACS 2013—Modelling and Simulation of Complex Systems: Stochastic and Deterministic Approaches*, ESAIM Proceedings and Surveys (EDP Sciences, Les Ulis, 2015), Vol. 48, pp. 364–384.
- C.-E. Bréhier, L. Goudenège, and L. Tudela, "Central limit theorem for adaptive multilevel splitting estimators in an idealized setting," in *Monte Carlo and Quasi-Monte Carlo Methods*, Springer Proceedings in Mathematics and Statistics Vol. 163 (Springer, Cham, 2016), pp. 245–260.
- C.-E. Bréhier, T. Lelièvre, and M. Rousset, "Analysis of adaptive multilevel splitting algorithms in an idealized case," *ESAIM Probab. Stat.* **19**, 361–394 (2015).
- J. Bucklew, *Introduction to Rare Event Simulation*. Springer Series in Statistics (Springer-Verlag, New York, 2004).
- F. Cérou, P. Del Moral, T. Furon, and A. Guyader, "Sequential Monte Carlo for rare event estimation," *Stat. Comput.* **22**(3), 795–808 (2012).
- F. Cérou, B. Delyon, A. Guyader, and M. Rousset, "On the asymptotic normality of adaptive multilevel splitting," *SIAM/ASA* **7**(1), 1–30 (2019).
- F. Cérou and A. Guyader, "Adaptive multilevel splitting for rare event analysis," *Stoch. Anal. Appl.* **25**(2), 417–443 (2007).
- F. Cérou, A. Guyader, T. Lelièvre, and D. Pommier, "A multiple replica approach to simulate reactive trajectories," *J. Chem. Phys.* **134**(5), 54–108 (2011).
- T. Dean and P. Dupuis, "Splitting for rare event simulation: A large deviation approach to design and analysis," *Stochastic Process. Appl.* **119**(2), 562–587 (2009).
- P. Del Moral and J. Garnier, "Genealogical particle analysis of rare events," *Ann. Appl. Probab.* **15**(4), 2496–2534 (2005).
- P. Dupuis, K. Spiliopoulos, and H. Wang, "Importance sampling for multiscale diffusions," *SIAM J. Multiscale Model. Simul.* **10**, 1–27 (2012).
- P. Dupuis, K. Spiliopoulos, and X. Zhou, "Escaping from an attractor: Importance sampling and rest points i," *Ann. Appl. Probab.* **25**(5), 2909–2958 (2015).
- G. Ferré and H. Touchette, "Adaptive sampling of large deviations," *J. Stat. Phys.* **172**, 1525 (2018).
- M. Garvels, D. Kroese, and J. van Ommeren, "On the importance function in splitting simulation," *Eur. Trans. Telecommun.* **13**(4), 363–371 (2002).
- P. Glasserman, P. Heidelberger, P. Shahabuddin, and T. Zajic, "Multilevel splitting for estimating rare event probabilities," *Oper. Res.* **47**(4), 585–600 (1999).

- ²⁷E. Gobet and G. Liu, "Rare event simulation using reversible shaking transformations," *SIAM J. Sci. Comput.* **37**(5), A2295–A2316 (2015).
- ²⁸A. Guyader, N. Hengartner, and E. Matzner-Løber, "Simulation and estimation of extreme quantiles and extreme probabilities," *Appl. Math. Optim.* **64**(2), 171–196 (2011).
- ²⁹H. Kahn and T. E. Harris, "*Estimation of Particle Transmission by Random Sampling*," Applied Mathematics Series 12 (National Bureau of Standards, 1951), pp. 27–30.
- ³⁰T. Lestang, F. Ragone, C.-E. Bréhier, C. Herbert, and F. Bouchet, "Computing return times or return periods with rare event algorithms," *J. Stat. Mech. Theory Exp.* **2018**(4), 043213 (2018).
- ³¹L. J. S. Lopes and T. Lelièvre, "Analysis of the adaptive multilevel splitting method on the isomerization of alanine dipeptide," *J. Comput. Chem.* **40**(11), 1198 (2019).
- ³²E. N. Lorenz, "Deterministic nonperiodic flow," *J. Atmos. Sci.* **20**(2), 130–141 (1963).
- ³³E. Louvin, E. Dumonteil, T. Lelièvre, M. Rousset, and C. Diop, "Adaptive multilevel splitting for Monte Carlo particle transport," *EPJ Nuclear Sci. Technol.* **3**(29), 29 (2017).
- ³⁴H. Louvin, "Development of an adaptive variance reduction technique for Monte Carlo particle transport," Ph.D. thesis (Université Paris-Saclay, 2017).
- ³⁵H. Louvin, E. Dumonteil, and T. Lelièvre, "Three-dimensional neutron streaming calculations using adaptive multilevel splitting," in *International Conference on Mathematics and Computational Methods Applied to Nuclear Science and Engineering (M&C 2017)*, Jeju, Korea (2017).
- ³⁶R. Poncet, "Méthodes numériques pour la simulation d'équations aux dérivées partielles stochastiques non-linéaires en condensation de Bose-Einstein," Ph.D. thesis (Université Paris-Saclay, 2017).
- ³⁷F. Ragone, J. Wouters, and F. Bouchet, "Computation of extreme heat waves in climate models using a large deviation algorithm," *Proc. Natl. Acad. Sci. U.S.A.* **115**(1), 24–29 (2018).
- ³⁸J. Rolland, "Extremely rare collapse and build-up of turbulence in stochastic models of transitional wall flows," *Phys. Rev. E* **97**(2), 023109 (2018).
- ³⁹J. Rolland, F. Bouchet, and E. Simonnet, "Computing transition rates for the 1-D stochastic Ginzburg-Landau-Allen-Cahn equation for finite-amplitude noise with a rare event algorithm," *J. Stat. Phys.* **162**(2), 277–311 (2016).
- ⁴⁰J. Rolland and E. Simonnet, "Statistical behaviour of adaptive multilevel splitting algorithms in simple models," *J. Comput. Phys.* **283**, 541–558 (2015).
- ⁴¹G. Rubino and B. Tuffin, "Introduction to rare event simulation," in *Rare Event Simulation Using Monte Carlo Methods* (Wiley, Chichester, 2009), pp. 1–13.
- ⁴²C. Schütte, S. Winkelmann, and C. Hartmann, "Optimal control of molecular dynamics using Markov state models," *Math. Program.* **134**(1), 259–282 (2012).
- ⁴³J. Skilling, "Nested sampling for general Bayesian computation," *Bayesian Anal.* **1**(4), 833–859 (2006).
- ⁴⁴J. Skilling, "Nested sampling for Bayesian computations," in *Bayesian Statistics 8*, Oxford Science Publication (Oxford University Press, Oxford, 2007), pp. 491–524.
- ⁴⁵I. Teo, C. Mayne, K. Schulten, and T. Lelièvre, "Adaptive multilevel splitting method for molecular dynamics calculation of benzamidine-trypsin dissociation time," *J. Chem. Theory Comput.* **12**(6), 2983–2989 (2016).
- ⁴⁶E. Vanden-Eijnden and J. Weare, "Rare event simulation of small noise diffusions," *Commun. Pure Appl. Math.* **65**(12), 1770–1803 (2012).
- ⁴⁷M. Villén-Altamirano and J. Villén-Altamirano, "RESTART: A method for accelerating rare events simulations," in *Proceeding of the Thirteenth International Teletraffic Congress*, Copenhagen, Denmark, June 19–26 of *Queueing, Performance and Control in ATM: ITC-13 Workshops* (North-Holland, Amsterdam, New York, 1991), pp. 71–76.
- ⁴⁸M. Villén-Altamirano and J. Villén-Altamirano, "RESTART: A straightforward method for fast simulation of rare events," in *Proceedings of the 1994 Winter Simulation Conference*, Orlando, 1994, pp. 282–289.
- ⁴⁹J. Wouters and F. Bouchet, "Rare event computation in deterministic chaotic systems using genealogical particle analysis," *J. Phys. A* **49**(37), 374002 (2016).